SAE TECHNICAL PAPER SERIES

983051

The Effects of Chassis Flexibility on Roll Stiffness of a Winston Cup Race Car

Lonny L. Thompson, Pipasu H. Soni, Srikanth Raju and E. Harry Law
Clemson Univ.

Reprinted From: 1998 Motorsports Engineering Conference Proceedings
Volume 1: Vehicle Design and Safety
(P-340/1)

The Engineering Society For Advancing Mobility Land Sea Air and Space®
INTERNATIONAL

Motorsports Engineering Conference and Exposition
Dearborn, Michigan
November 16-19, 1998

400 Commonwealth Drive, Warrendale, PA 15096-0001 U.S.A. Tel: (724) 776-4841 Fax: (724) 776-5760

ISSN 0148-7191

Printed in USA

983051

The Effects of Chassis Flexibility on Roll Stiffness of a Winston Cup Race Car

Lonny L. Thompson, Pipasu H. Soni, Srikanth Raju and E. Harry Law
Clemson Univ.

ABSTRACT

Predictable handling of a racecar may be achieved by tailoring chassis stiffness so that roll stiffness between sprung and unsprung masses are due almost entirely to the suspension. In this work, the effects of overall chassis flexibility on roll stiffness and wheel camber response, will be determined using a finite element model (FEM) of a Winston Cup racecar chassis and suspension. The FEM of the chassis/suspension is built from an assembly of beam and shell elements using geometry measured from a typical Winston cup race configuration. Care has been taken to model internal constraints between degrees-of-freedom (DOF) at suspension to chassis connections, e.g. at ball and pin joints and internal releases.

To validate the model, the change in wheel loads due to an applied jacking force that rolls the chassis agrees closely with measured data. The roll stiffness predicted from finite element models of the front and rear suspension compared closely to those calculated using a rigid-body kinematics model. To study the effects of chassis flexibility on roll, torsional stiffness is increased by adding strategic members to the chassis structure. Results from the finite element analysis indicate that the effective roll stiffness of the front suspension interacting with the chassis, increased by 7.3 % over a baseline chassis when the chassis torsional stiffness was increased by 130% over a baseline chassis stiffness of 9934 ft-lb/deg. As the chassis stiffness is increased further above this value, the front roll stiffness changed very little. From these results, the minimum torsional stiffness required so that the effective roll stiffness of the front suspension is within 3 % from the roll stiffness with a rigid chassis, is about 23100 ft-lb/deg.

INTRODUCTION

Race teams have found that if they can reduce the twist in the chassis by increasing the torsional rigidity, they can control the handling of the car better [1]. Increased torsional stiffness improves vehicle handling by allowing the suspension components to control a larger percentage of a vehicle's kinematics. Teams competing in the Winston Cup racing series typically purchase their basic chassis from one of two manufacturers - Hopkins or Laughlin. These base chassis, sometimes referred to as “roller chassis”, are then modified by adding structural members for improved strength or stiffness [2]. Some teams build their own chassis from the ground-up. In any case, when designing a new chassis or modifying a base Hopkins or Laughlin chassis, structural members must be strategically located in order to reduce twist of the frame and minimize local deflections of suspension support points. In order to reduce twist and deflections of suspension support points, a minimum level of chassis stiffness must be achieved, while at the same time keeping the overall weight to a minimum. An important question is then, “what minimum stiffness value should the chassis be designed for in order to control lateral load transfer?"

In order to help answer this question finite element models of the chassis and suspension may be used to predict changes in roll and camber response due to differential load inputs. Structural finite element models (FEM) of Laughlin, Hopkins and other Winston Cup chassis have been developed in [3,4]. These structural models use beam elements for the tubular and box beam frame members and thin shell elements for the floor pan and firewall sheet metal. These models are currently being used to evaluate torsional stiffness of competing chassis designs [2], and aid in the design of a twist fixture used to measure torsional stiffness [5]. In this work, the chassis models are combined with front and rear suspension finite element models to study the interaction between the suspension and the chassis. By modeling the chassis/suspension interaction, we quantify the effective roll, and wheel camber response as a function of chassis stiffness. Torsional stiffness is increased by adding strategic members to the chassis structure. Results from the finite element analysis will help answer the question of how stiff the chassis needs to so that roll stiffness between sprung and unsprung masses are due almost entirely to the suspension. Other results from the chassis/suspension model give insight into questions such as the contribution of individual components (chassis and suspension members) to the overall stiffness of the vehicle.

The main objective of this work is to develop a finite element model of a typical suspension set-up and chassis for a Winston Cup racecar. This model will be used to determine the effects of chassis flexibility on roll stiffness and wheel camber response due to differential load inputs. In particular, the FE model will be used to determine the:

- Roll stiffness of the front and rear suspensions with rigid chassis and verify finite element results with a rigid-body kinematics model.
- Individual contributions of the front suspension components to roll stiffness including the sway bar and coil springs.
- Individual contributions of the rear suspension components to roll stiffness including truck arms, truck arm/chassis connections, and coil springs.
- Effective roll stiffness and camber angle changes of the front and rear suspension with flexible chassis.
- The minimum torsional stiffness required so that the effective roll stiffness is within 3 % from the roll stiffness with a rigid chassis.

SUSPENSION DESIGN FOR A WINSTON CUP RACECAR

The main components of a Winston Cup racecar are the chassis and the front and rear suspensions, see Figure 1. The main function of the chassis involves safety of the driver (main cage) and the placement of suspension and other components (front and rear clips). The members of the chassis are constructed primarily of box-beam and tubular members, which are specified by the National Association of Stock Car Auto Racing, NASCAR [6]. The front suspension is located under the front clip of the chassis. The front suspension components includes the upper and lower A-arms (control arms), tire and wheel assemblies, spindles, compression springs, shock absorbers, the sway bar assembly, and steering assembly, see Figure 2.

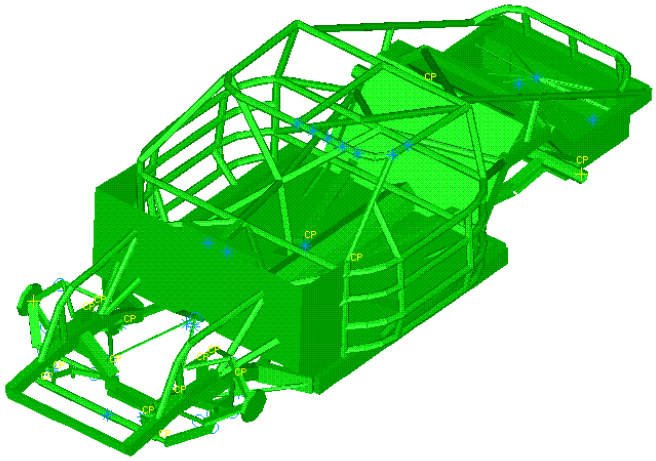

Figure 1. Winston Cup chassis and suspension

Compression springs are mounted between the lower A-arms and spring perches on the chassis. The upper spring perch, integrated with the box-beam frame rails, allows for vertical adjustment of the springs using a threaded rod. Through NASCAR rules, the use of an integrated shock/spring assembly is not permitted; therefore the shock and spring are separate components [6]. NASCAR rules also specify a 110-inch wheelbase, no adjustable A-arms, and a maximum of one shock absorber per wheel [6]. The sway bar assembly includes the sway bar, sway bar arms, and pivot links. The sway bar is mounted using bushings in a transverse tube to the front end of the front clip. The sway bar is free to rotate about its principal axis. The sway bar arms connect the sway bar to the lower A-arms with pivot links.

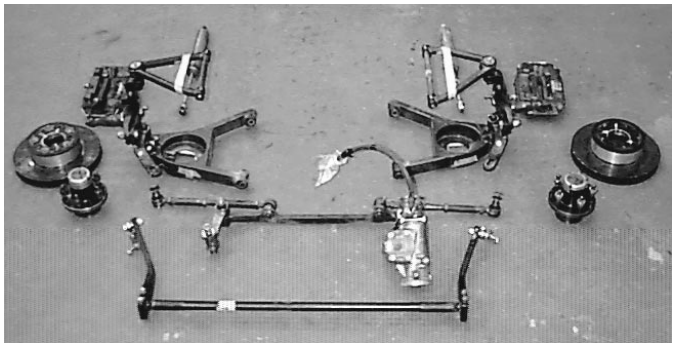

Figure 2. Components of the front suspension

The rear suspension consists of two trailing I-beam (truck) arms running from a solid axle to the chassis (under the main cage) and a panhard bar running from the rear axle to the chassis (rear clip). Figure 3 shows the components of the rear suspension. The truck arms are connected to the rear axle through the use of U-bolts at one end, and with pin connections to the chassis at the other end. The rear compression springs act in a similar manner as the front springs. These springs are connected to the truck arms and through spring perches to the chassis. The panhard bar provides lateral restraint between the chassis and the rear axle. The vertical position to the chassis and length of the panhard bar are adjustable. The vertical position of the chassis/truck arm connection can also be adjusted.

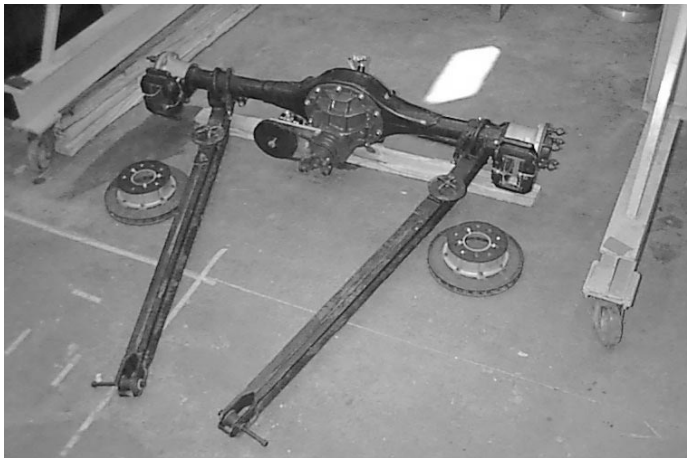

Figure 3. Components of the rear suspension

FINITE ELEMENT MODEL OF CHASSIS WITH SUSPENSION

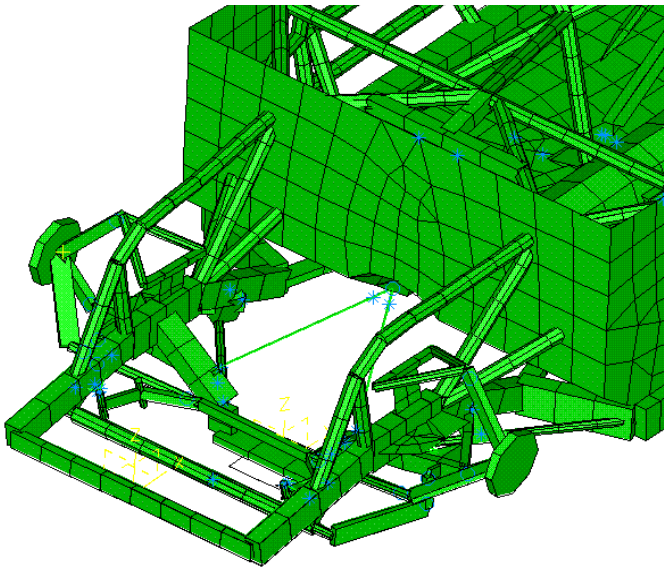

Figure 4. Finite element model of front suspension and chassis

The chassis/suspension model was constructed using I-DEAS software from SDRC [7], see Figure 4. The geometry of the chassis and suspension model is based on measured data taken from a Hopkins chassis supplied by one of the race teams [8]. The chassis was measured by projecting the centers of the welded joints onto a surface plate to determine the x-y components of key-point positions. The heights of the key-points above the surface plate were measured to determine the z-coordinates. The chassis model is constructed using beam elements for the tubular members of the roll cage and front and rear clips. Thin shell elements are used to model the floor pan and firewall. The frame rails are also modeled with beam elements.

The front suspension includes the upper and lower A-arms (control arms), compression springs, spindles, wheel hubs and sway bar assembly. Tire stiffness is not modeled. The sway bar assembly includes the sway bar, sway bar support arms, and pivot links. The model also includes the steering assembly including the idler and pit man arms, tie rod and drag link. The finite element model of the front suspension assembly is shown in Figure 5. Beam elements are used to model most of the suspension components. The spring mount platform on the lower A-arms is modeled with shell elements. The coil springs are modeled with linear spring elements and connected between the lower A-arm and upper spring mounts. The rear suspension model shown in Figure 6 consists of the rear axle, truck arms, springs, and panhard bar. Both the chassis and suspension models are constructed of steel with Young's modulus E = 30 x 10^6 psi, and Poisson's ratio ν = 0.3.

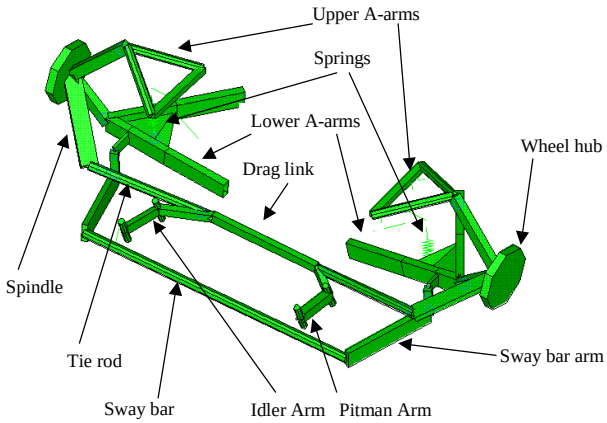

Figure 5. Finite element model of front suspension

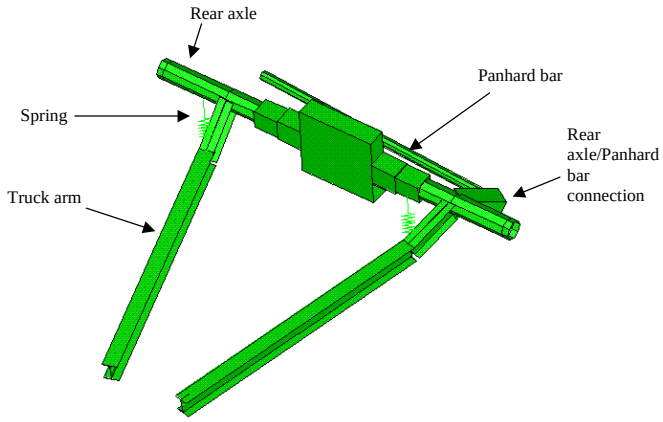

Figure 6. Finite element model of rear suspension

The suspension geometry is specified in the global co-ordinate system illustrated in Figure 7. The origin of this co-ordinate system is at the intersection between the centerline of the car and a perpendicular line through the right front wheel hub. The vertical position of the origin is located at ground height. The x-axis is directed along the longitudinal direction from front to rear along the centerline of the car, the y-axis is oriented in the lateral direction with positive directed to the right and passing through the front wheel centers, and the z-axis is in the vertical direction (positive up).

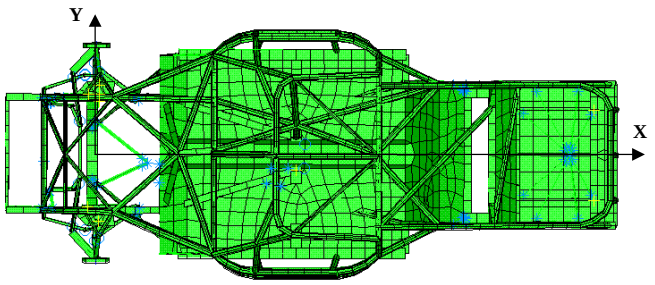

Figure 7. Global Co-ordinate System

Care has been taken to model internal constraints between degrees-of-freedom (DOF) at suspension connections. Constraints between DOF at joints and internal releases are modeled to simulate the connection between the chassis and suspension. To connect the suspension to the chassis, local coordinate systems and coupled degrees-of-freedom are employed. In the front, local coordinate triads are placed at the pit man arm, idler arm, upper and lower A-arms, and sway bar connections to the chassis. Figure 8 shows the finite element model of the upper A-arm connection to the spring perch bracket using coupled degrees-of-freedom to model a hinge joint. The coil spring is modeled with a linear spring element connecting the lower A-arm to the upper spring perch. For simplicity, the spring perch is modeled with a rigid plate with a large thickness dimension, see Figure 9. The effects of local plate thickness for a detailed model of the front spring perch on roll stiffness, and wheel camber and steer is reported in [9]. In the rear, local coordinate triads are placed at the truck-arm attachments together with coupled degrees-of-freedom. Further details on the suspension model and connections to the chassis are given in [10].

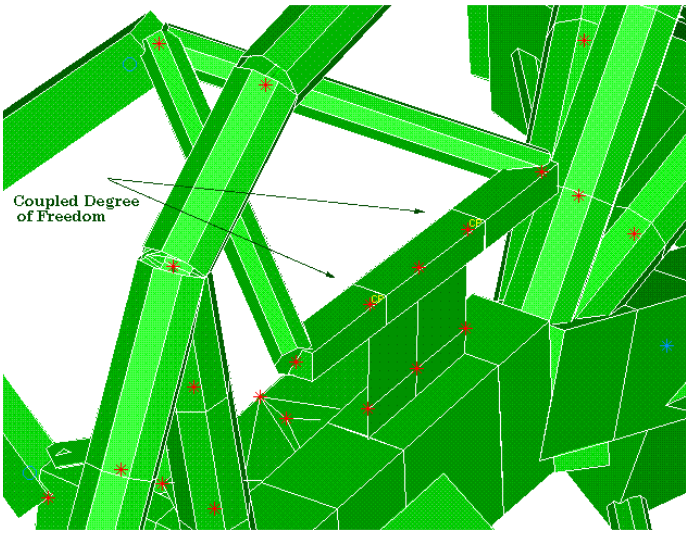

Figure 8. Finite element model of upper A-arm connection to spring perch bracket using coupled degrees-of-freedom to model hinge joint.

The following assumptions were made for the chassis/suspension model:

- The material is assumed linear elastic and calculations are performed using linear static finite element analysis with small deformations resulting in constant stiffness predictions.
- The coil springs are modeled using linear spring elements with constant spring rates.
- The wheel travel due to vertical inputs is small resulting in small deflections from the design position.

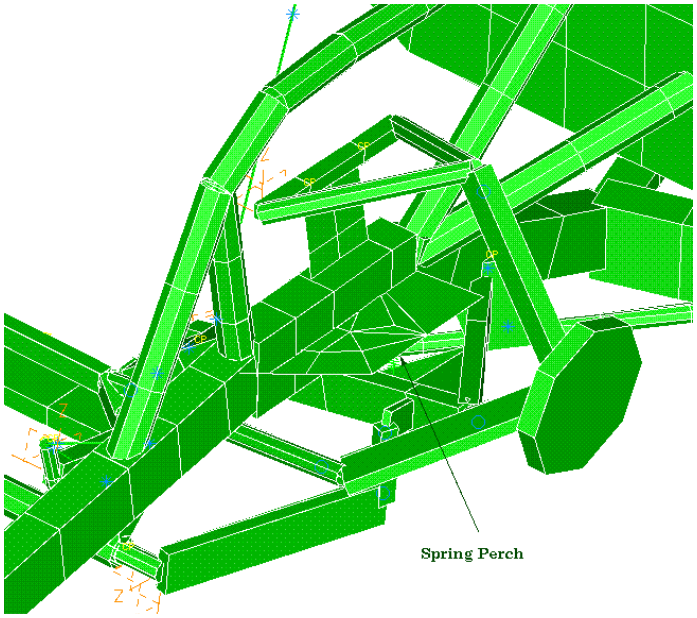

Figure 9. Finite element model of spring perch. Local coordinate triads illustrated for upper A-arm, and sway bar. Linear spring element representing coil spring is connected between lower A-arm and upper spring perch.

VALIDATION OF MODEL

To verify the chassis/suspension FEM model, results from a static “jack test” are compared to measured data. The “jack test” consists of applying a vertical load using a hydraulic jack on the left frame rail of the chassis, simulating a vehicle roll to the right as occurs in a left-hand turn [8]. For the test, the spring rates were set as follows: left front = 761 lb_f/in, right front = 764 lb_f/in, and left rear = right rear 166 lb_f/in. For this test, the sway bar rate is set at 792.9 lb_fÞin/deg, which corresponds to a sway bar diameter of 1.1 in. In the finite element model, rigid elements have been projected from the wheel hubs vertically down to the ground to account for tire offset. Boundary conditions for the finite element model consist of the following: left front tire base restrained in u_y, u_z translations; left rear tire base restrained in u_x, u_y, u_z translations; and right front and rear tire bases restrained in u_z translation. The “jack” force was placed at the position **x** = (63.0,-34.5,4.5) inches. In the finite element model, this point is located approximately 7.3 inches in the lateral direction from the neutral axis of the left frame rail. To accommodate this offset, two rigid elements were used to connect the load application point to the beam elements modeling the frame rail, see Figure 10.

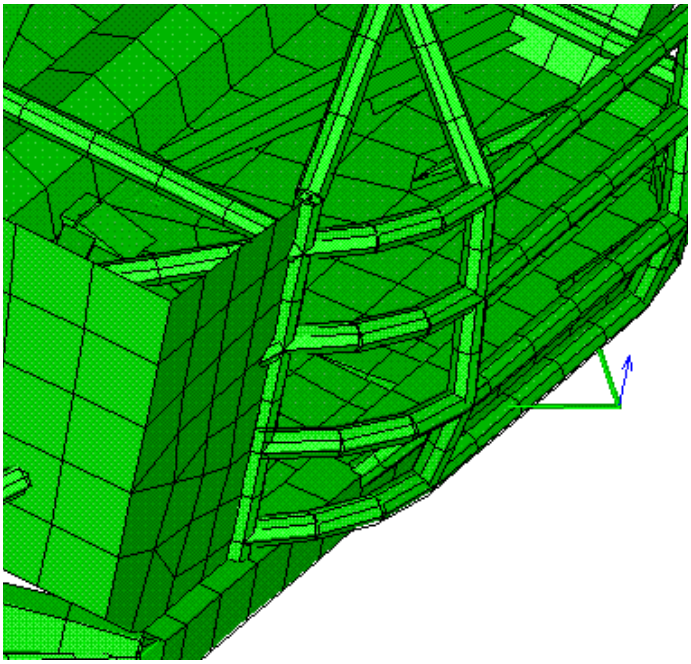

Figure 10. Jack test load application point attached to chassis with rigid elements.

The changes in normal wheel load due to the jack force for the front tires predicted from the FEM compared to actual test data and predictions from a rigid-body-kinematics model is shown in Figures 11 through 12. These results show excellent agreement between the FEM and measured data with a maximum error less than 5 %.

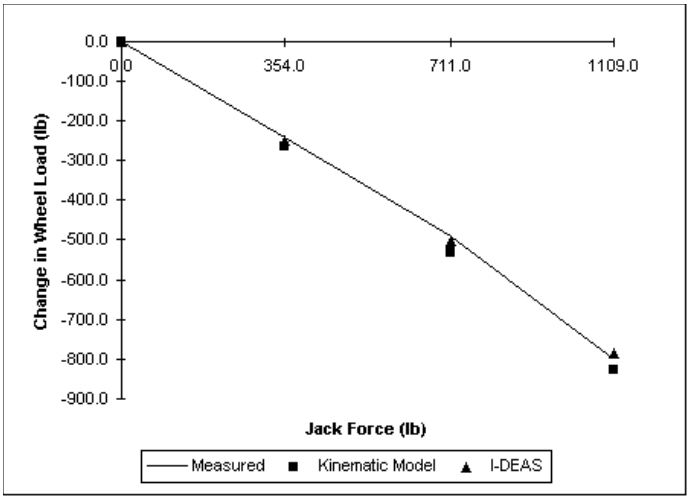

Figure 11. Left front change in wheel load versus jack force

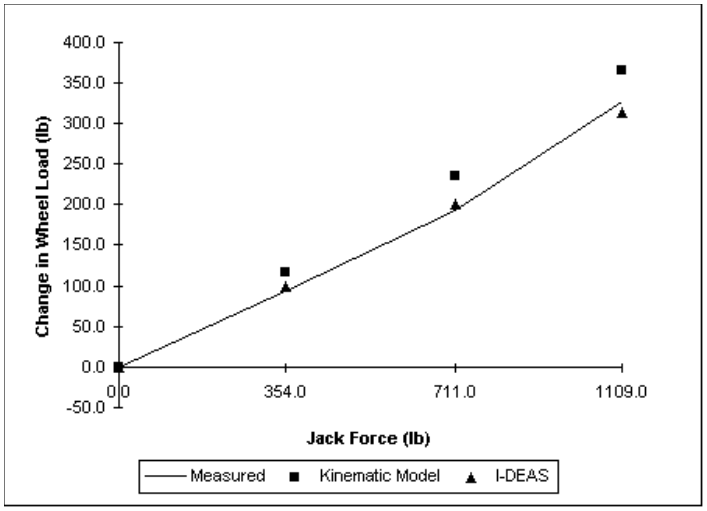

Figure 12. Right front change in wheel load versus jack force

ROLL AND CAMBER OF FRONT SUSPENSION WITH RIGID CHASSIS

In this section, the roll stiffness and camber response due to differential load inputs of the front suspension with a rigid chassis is calculated. The roll stiffness and camber of the front suspension is controlled primarily by: (1) the right/left coil springs which connect the lower A-arms to the chassis mounts, and (2) the sway-bar across the front clip, and to a lesser extent, the compliance of the suspension structural members themselves. In order to compare roll stiffness results with a rigid-body kinematics model developed in [8], the spring rates are set at (left front = 2000 lb/in, right front = 1200 lb/in). The sway bar rate is 556.4 in-lb/deg corresponding to a diameter of 1.0 in. In order to determine the front roll stiffness and camber response, the locations of the wheel hubs, H, and wheel spindles, S, were measured for a typical Winston Cup race car at ride height [8]. The locations of these points, in the global coordinate system, are given in Table I and are shown in Figure 13.

Table I. Hub and Spindle Co-ordinates for Left and Right Wheels.

Description	Co-ordinates (inches)		
	X	Y	Z
Left front outer hub	-0.2269	-30.033	13.2996
Left front inner spindle	-0.2269	-29.035	13.3662
Right front outer hub	-0.0171	30.4338	13.6749
Right front inner spindle	-0.0171	29.4359	13.6100

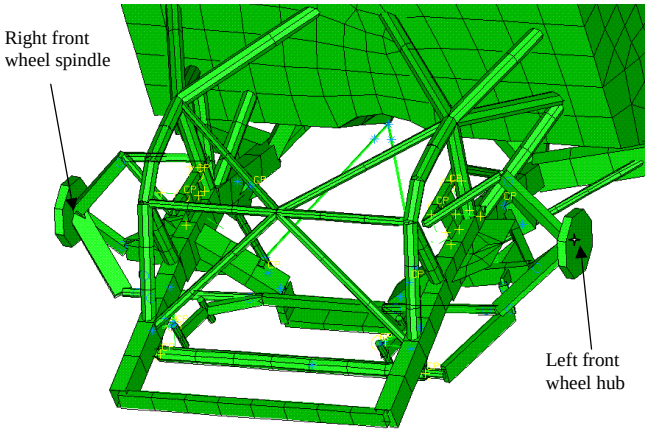

Figure 13. Location of wheel hub and spindle centers

Symmetry is not present between the left and right hand coordinates due to the initial roll of the chassis at race height.

The following boundary conditions are applied to the model for the analysis of front suspension with rigid chassis.

- Equal and opposite forces are applied at the front wheel hub centers, producing a torque; see Figure 14. Results for roll and camber change by less than 1% using differential inputs in the opposite direction.
- Coupled DOF between the suspension and chassis are restrained.

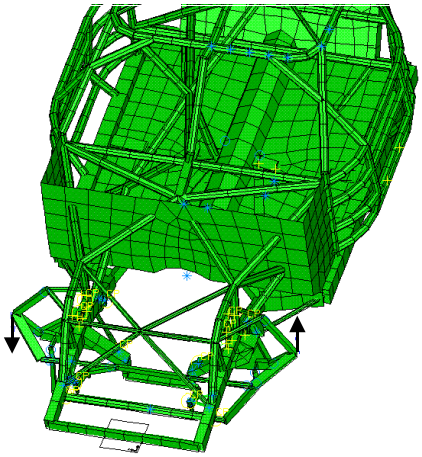

Figure 14. Applied torque with equal and opposite forces applied at wheel hubs

FRONT ROLL STIFFNESS – In order to calculate roll stiffness, the vertical deflections v_L and v_R of the front wheel hub points, are determined for the driver's (left) and the passenger's (right) side respectively. The applied torque is calculated from $T = F \cdot d_R$ = 5039 ft-lb, where d_R = 60.47 inch, is the lateral distance between wheel hub centers (front track width). The roll angle of the left front wheel hub, ϕ_L and the right front wheel hub, ϕ_R are calculated as,

$$\phi_R = \arctan\left[\frac{v_R}{d_R/2}\right] \quad (1)$$

$$\phi_L = \arctan\left[\frac{v_L}{d_R/2}\right] \quad (2)$$

The average roll angle is calculated as,

$$\phi = \left(\frac{\phi_L + \phi_R}{2}\right) \quad (3)$$

The roll stiffness K_R, is then calculated using the equation,

$$K_R = \frac{F \cdot d_R}{\phi} \quad (4)$$

CAMBER – Camber is an important parameter in the handling of a racecar. Tire camber is a function of the vertical displacement of the chassis and the steer angle of each tire [8]. The sign convention for camber is such that positive camber results in the top of the tire tilting outward from the vehicle centerline and negative camber results in the tire tilting inward. Defining the wheel local vertical as the line from the wheel hub center to the 'top' point on the outside edge of the wheel/tire, the camber γ, represents the angle between the global vertical line and the wheel local vertical. Camber is calculated using the co-ordinates of the wheel center H (the hub) and wheel spin axis point S (the spindle) for each wheel. The camber angle, γ, can be calculated as [8]:

$$\gamma = \arcsin\left(\frac{S_z - H_z}{\sqrt{(S_x - H_x)^2 + (S_y - H_y)^2 + (S_z - H_z)^2}}\right) \quad (5)$$

This expression ensures the correct sign of the camber angle. If this value is negative then the camber is negative, and the top of the tire is tilted inward toward the centerline of the car. If γ is positive then the camber is positive, and the top of the tire is tilted away from the centerline. The x-components are included in the above expression to account for possible steer/toe ("yaw") angles. The initial camber is calculated using Eq. 5, with the initial co-ordinates of the front hub and spindle points, given in Table I. The initial camber for the left tire is, γ = +3.82°. The initial camber for the right tire is, γ = -3.72°. The final camber is calculated using the same equation from the deformed co-ordinates of the front hub and the spindle points. The difference between the final and the initial camber values give the value of camber change, $\Delta\gamma$.

Camber response to differential load input is given by $1/K_C$, where

$$K_C = \frac{F \cdot d_R}{|\Delta\gamma|} \tag{6}$$

is the "camber stiffness". With this geometry, linear spring rates, sway bar, and compliant suspension members, the roll stiffness due to differential vertical load inputs at the wheel hubs is K_R = 1955 ft-lb/deg. The roll stiffness of the front suspension predicted by the rigid-body kinematics model given in Day [8] is K_R = 2019 ft-lb/deg. The difference between the roll stiffness calculations based on the compliant finite element suspension model and the rigid-body kinematics model is less than 2.4%. Table II summarizes the roll stiffness and the wheel angles due to the applied torque as predicted by the suspension with fixed constraints at the chassis coupled DOF.

Table II. Front Roll Stiffness and Camber Response for Rigid Chassis/Suspension Model

Rigid Chassis/Suspension Model	
Suspension Roll Stiffness (ft-lb/deg)	1952
Right Front Camber Stiffness (ft-lb/deg)	-3100
Left Front Camber Stiffness (ft-lb/deg)	2651
Right Front Camber change (deg)	-1.625
Left Front Camber change (deg)	1.901
Roll Angle (deg)	-2.577

The contribution to roll stiffness of the flexible suspension members including the A-arms and links is found by increasing the Young's modulus (E) in these members. By increasing the modulus, the suspension members approach the rigid case. The modulus of elasticity was varied between E = $3x10^7$ psi and E = $3x10^9$ psi. To determine the contribution from the coil springs to the front roll stiffness, the sway bar assembly (which includes the sway bar, sway bar arms and pivot links) is removed from the model and the roll stiffness is calculated. In this way, the contribution to roll stiffness from the springs in combination with the support members is determined, without sway bar. To determine the contribution from the sway bar assembly, the front coil springs are removed from the model. In this way, the contribution to roll stiffness of the flexible sway bar in combination with the support members is determined, without springs.

From the results shown in Table III, the springs contribute 59 % of the total front roll stiffness while the sway bar assembly contributes 41 %. By increasing the stiffness of the suspension members, the corresponding roll stiffness increases by less than 4 %. This indicates that the compliant front suspension members are approximately rigid in the FEM.

Table III. Summary of Front Roll Stiffness Values. Spring rates (LF = 1200 lb/in, RF = 2000 lb/in)

Model	**K (ft-lb/deg)**
FEM (E = 3e7 psi)	1952
FEM (E = 3e9 psi)	2025
Rigid Kinematics [8]	2019
Springs	1182
Sway Bar	839

ROLL AND CAMBER OF FRONT SUSPENSION WITH FLEXIBLE CHASSIS

In this section, the effects of chassis flexibility on roll stiffness and camber response are studied. Several chassis stiffness cases are studied based on the different structural modifications to the baseline Hopkins chassis made in [2]. Effective front roll stiffness and camber response of the suspension with flexible chassis is determined based on differential vertical load inputs at the front wheel hub centers. The model allows for small deflections only and predicts changes in roll stiffness and camber response due to changes in chassis stiffness. Specifically, the vertical wheel travel allowed due to the vertical inputs is small resulting in camber response due to changes in stiffness. For this effective front roll stiffness calculation, only the front suspension and chassis model is used while the rear suspension is disconnected. The two rear spring mounts are constrained in all translations and in y and z rotation. ($u_x = u_y = u_z = 0$, $\theta_z = \theta_y = 0$, and θ_x = free). These boundary conditions are representative of constraints applied by a twist fixture used by several race teams to measure torsional stiffness [3]. Recent studies given in [5] have shown that these restraints at the rear spring perches are "over-constrained" leading to torsional stiffness predictions which are elevated by 9% over the minimum constraint condition. However, for the purposes of this study, use of the boundary conditions described above is sufficient to predict relative changes in roll and camber response due to changes in chassis stiffness.

DESCRIPTION OF STRUCTURAL MODIFICATIONS – Nine structural changes are considered based on the different modifications to the baseline Hopkins chassis given in [2]. Changes in chassis torsional stiffness, and effective roll stiffness and camber response of the suspension with flexible chassis are compared with these different configurations and also the rigid chassis configuration. In the following, the nine cases considered are described.

Case 1: Baseline Hopkins chassis – The baseline Hopkins chassis with the front suspension model is shown in Figure 15. The torsional stiffness for this configuration calculated for the bare chassis is K = 9934 ft-lb/deg. The

base Hopkins chassis in combination with the front suspension has an effective roll stiffness of K_R = 1759 ft-lb/deg. This roll stiffness value can be compared to the rigid chassis value of K_R = 1952 ft-lb/deg. The flexibility of the baseline Hopkins chassis reduces the roll stiffness by 10%. The stiffness values for the baseline Hopkins chassis/suspension model are summarized in Table IV.

Table IV. Torsional Stiffness, Roll Stiffness and Camber Response due to differential load inputs. (ft-lb/deg)

Chassis Torsional Stiffness	9934
Chassis/Suspension Roll Stiffness	1759
Camber Stiffness (Left)	2335
Camber Stiffness (Right)	2726

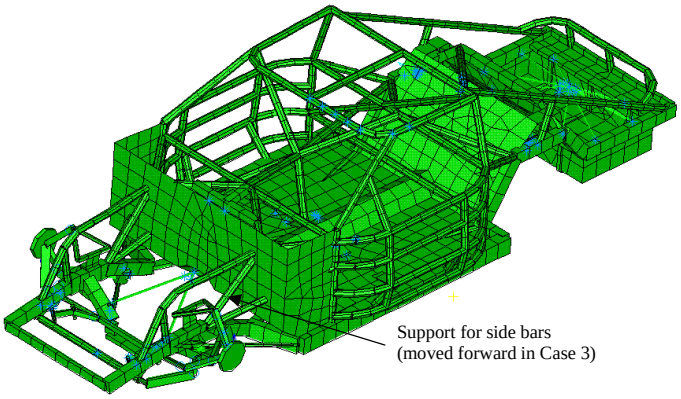

Figure 15. The baseline Hopkins chassis FEM with front suspension

Case 2: A-Bar Added to the Front Clip – In this case a vertical A-bar is added to the front clip. The A-bar is standard structural tubing with dimensions 1.0" OD and 0.035" wall thickness. A horizontal supporting bar with 1.0" OD and 0.049" wall thickness was also added as shown in Figure 16.

Case 3: Engine Bay Triangle – In this case, the support bars shown in Figure 15, are moved forward of the fire wall and positioned vertically as shown in Figure 16. A triangle configuration of standard 1.0" OD and 0.035" wall thickness structural tubing is added in the engine bay area as shown in Figure 16.

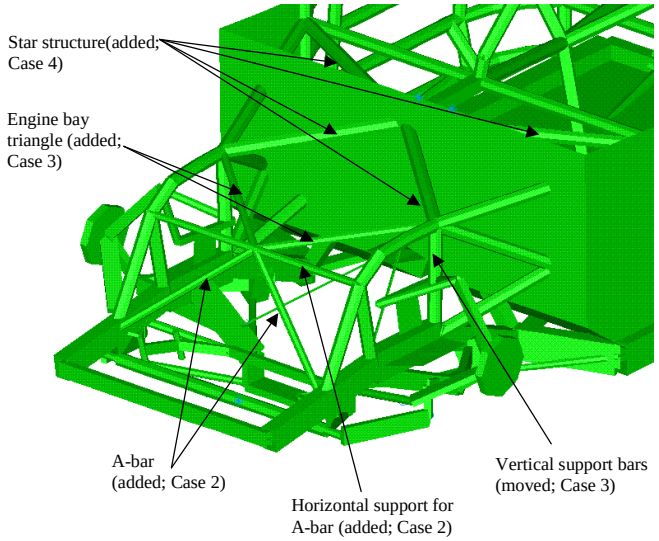

Figure 16. Structural Modifications to a Baseline Hopkins Chassis

Case 4: Star Structure, X-Structure Modifications – In this case, side and horizontal support bars are removed and a V-bar consisting of standard structural tubing, 1.75" OD and 0.065" wall thickness, is added in the engine bay area. A horizontal V-bar, 1.75" OD and 0.065" wall thickness is added in the region behind the fire wall to form a star structure in the transition region as shown in Figure 16. The bent side tubes are straightened and the lower A-arm support bars are stiffened by changing their dimensions from 1.0" OD and 0.12" wall thickness to 1.5" OD and 0.12" wall thickness.

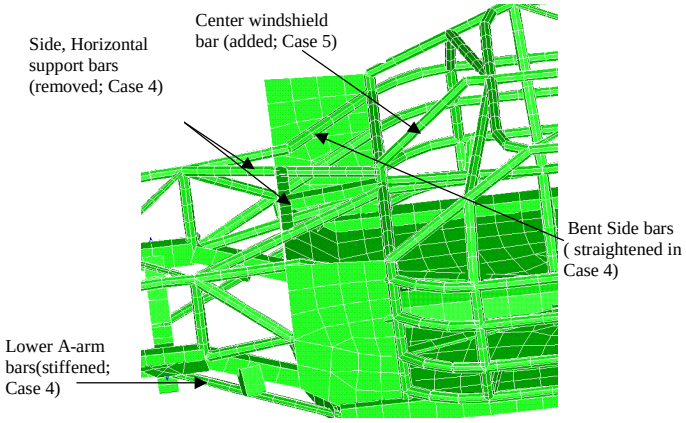

Figure 17. Structural Modifications to a Baseline Hopkins Chassis

Case 5: Center Windshield Bar – In this case, a center windshield bar with standard 1.75"OD and 0.065" wall thickness extends forward from the center of the roof, and down to a lateral support bar under the dash as shown in Figure 17.

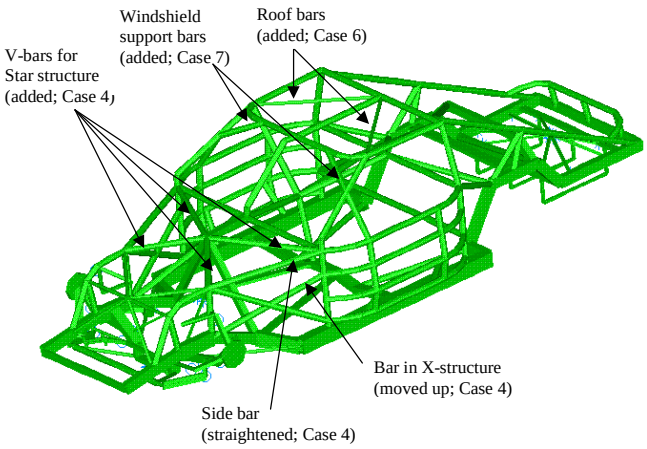

Figure 18. Structural Modifications to a Baseline Hopkins Chassis (Sheet Metal Removed for Clarity)

Case 6: Roof Bars – In this case, diagonal roof bars of 1.0" OD and 0.065" thickness are added as shown in Figure 18.

Case 7: Windshield Support Bars – In this case, windshield support bars of 1.75" OD and 0.065" wall thickness are added to the front windshield as shown in Figure 18.

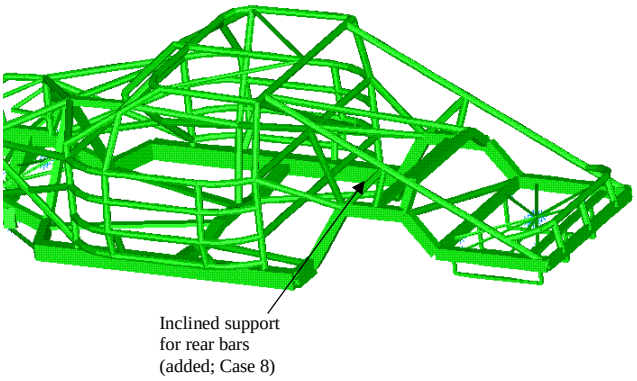

Figure 19. Structural Modifications to a Baseline Hopkins Chassis. (Sheet Metal Removed for Clarity)

Case 8: Rear Support Bars – In this case, support bars of 1.75"OD and 0.065" wall thickness are added in the rear, as shown in Figure 19.

Case 9: Vertical V-Bar Behind Fire Wall – In this case, a vertical V-bar made of rectangular cross section 1.75" base x 1.75" height x 0.077" wall thickness is added immediately behind the firewall, as shown in Figure 20. This chassis configuration is similar to the final design of [2].

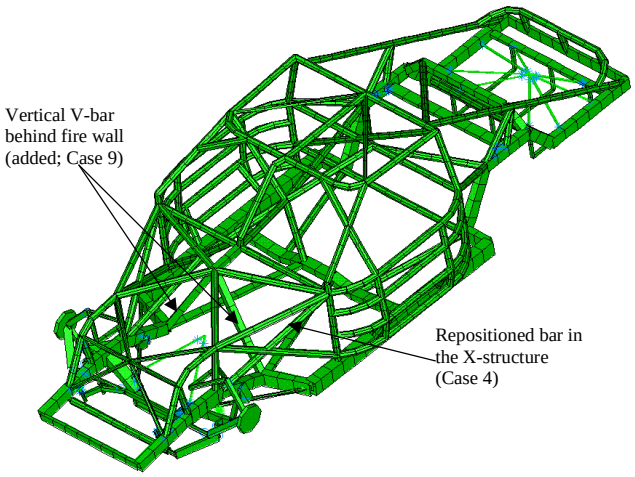

Figure 20. Diagram Indicating Structural Modifications to a Baseline Hopkins Chassis. (Sheet Metal Removed for Clarity)

TORSIONAL STIFFNESS – Comparisons of torsional stiffness values based on the constraints described earlier for the nine different chassis configurations are given in Table V and Figure 21.

Table V. Comparison of Torsional Stiffness

Case	K ft-lb/deg	Increase over nominal (%)
1	9934	0
2	11102	12
3	14845	49
4	19953	101
5	20460	106
6	23100	133
7	24662	148
8	25001	152
9	32943	232

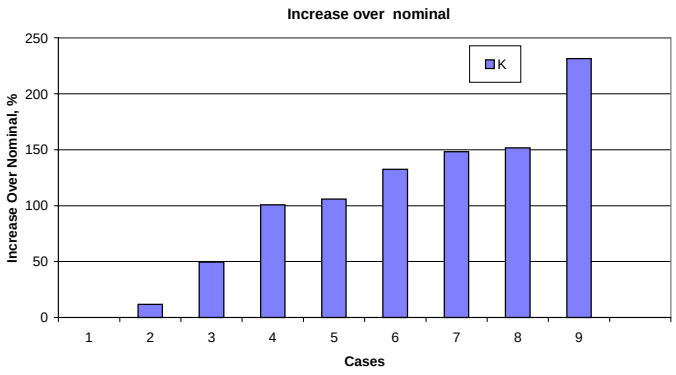

Figure 21. Percentage Increase in Torsional Stiffness over Nominal

Results show that the changes made in Cases 3, 4, and 9, i.e., the engine bay triangle, star structure and V-bar structure behind the fire wall, had the largest increase in torsional stiffness. The addition of the center windshield bar (Case 5) and the rear support bars (Case 8) have the least influence on torsional stiffness. With the constraints described earlier, the torsional stiffness value of the final configuration in Case 9 is increased by 231% over the baseline value of 9934 ft-lb/deg.

EFFECTIVE ROLL STIFFNESS – Comparisons of effective roll stiffness of the front suspension interacting with the flexible chassis are given in Table VI and Figure 22.

Table VI. Comparison of Effective Roll Stiffness due to differential load inputs.

Case	K_R ft-lb/deg	Increase over nominal (%)	Decrease from Rigid (%)
1	1759	0.0	9.9
2	1764	0.3	9.6
3	1799	2.9	7.8
4	1859	5.7	4.8
5	1861	5.8	4.7
6	1887	7.3	3.3
7	1894	7.7	3.0
8	1895	7.7	2.9
9	1904	8.3	2.4

The percentage decrease in the roll stiffness from the rigid chassis for different configurations is shown in Figure 23. The largest relative increase in roll stiffness occurred with the addition of the engine bay triangle (2% relative increase) and with the addition of the star structure (3.4% relative increase). This relatively large change in roll stiffness was expected since the torsional stiffness of the chassis increased substantially with these modifications. With the addition of the diagonal bars on the roof in Case 6, the roll stiffness increased another 1% to K_R = 1887 ft-lb/deg, which is a 7.3% increase over the baseline value, and within 3% of the rigid chassis value. As the chassis stiffness is increased above K = 23100 ft-lb/deg, the effective roll stiffness changed very little, even with the large stiffness increase from adding the V-bar structure behind the fire wall. Thus, to stabilize the effective roll stiffness, a chassis torsional stiffness of about 130% above the nominal value is required. Increasing the chassis stiffness above this value does not significantly change the effective roll stiffness. The roll stiffness of the final chassis configuration is only 2.4 % lower than the rigid chassis configuration, whereas the baseline configuration is 9.9 % lower.

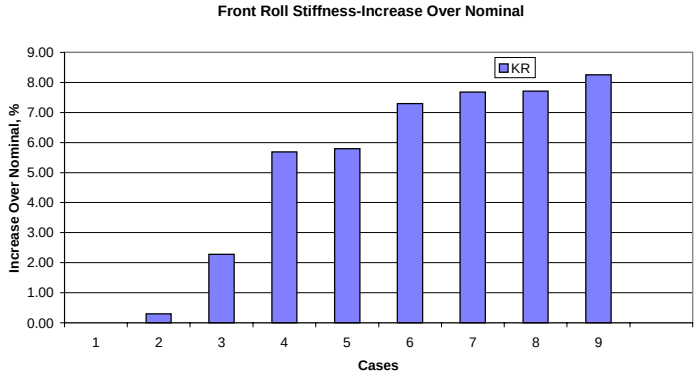

Figure 22. Percentage Increase in Roll Stiffness over Nominal for Different Configurations

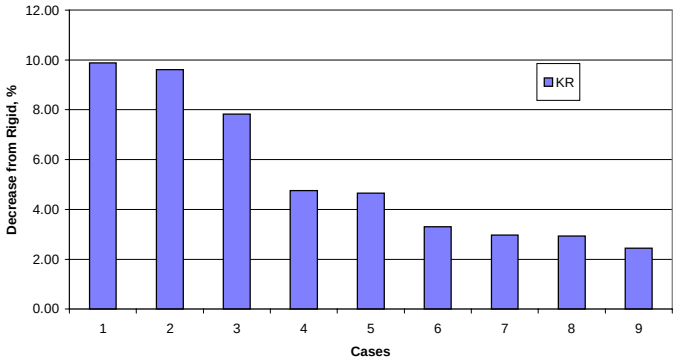

Figure 23. Percentage Decrease in Roll Stiffness from Rigid Chassis Configuration

WHEEL CAMBER – The change in camber angle due to the applied torque input for the different chassis configurations relative to the baseline chassis is given in Figure 24, while the change from the rigid chassis case is given in Figure 25. The change in camber response follows the same trend as the effective roll stiffness. For the baseline chassis, the deviation of the camber angle from the rigid chassis configuration is 13%. The greatest increase in camber response occurs during Cases 3, 4, and 6, corresponding to the addition of the engine bay triangle, star-structure, and roof bars, respectively. For Case 6, the camber angle for the left wheel has changed by 9.6 % and for the right wheel the change is 10.6 % from the baseline chassis. As the chassis stiffness is increased beyond 23100 ft-lb/deg, the camber does not change significantly. The camber angle change corresponding to a chassis of 23100 ft-lb/deg is within 2.5 % of the camber change for the rigid chassis. Beyond this value, the camber angle change approaches the camber value for the rigid chassis asymptotically. Thus it appears that a chassis stiffness of about 130% over baseline is sufficient to control both roll and camber.

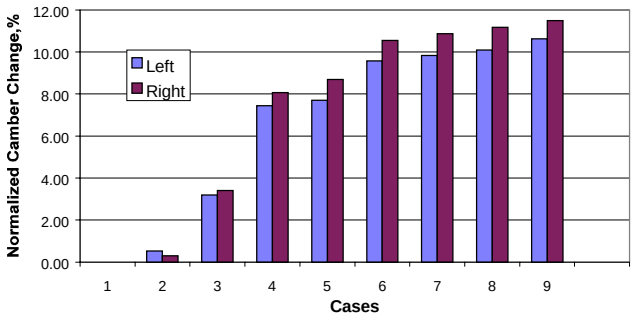

Figure 24. Percentage Increase in Left and Right Camber Response $|\Delta\gamma|$, from Nominal Chassis Configuration.

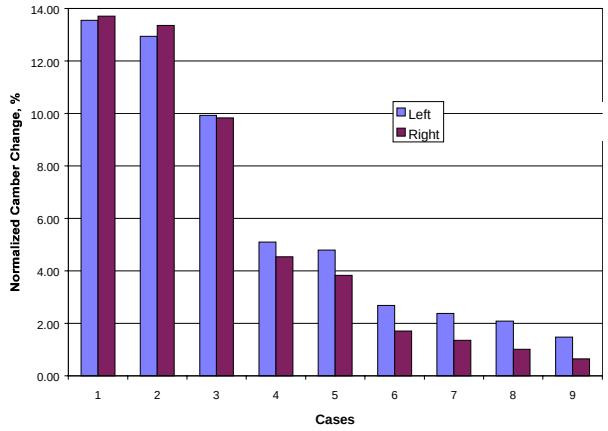

Figure 25. Percentage Decrease in Left and Right Camber Response $|\Delta\gamma|$, from Rigid Chassis Configuration.

ROLL STIFFNESS OF REAR SUSPENSION WITH RIGID CHASSIS

In this section, the roll stiffness of the rear suspension is examined. The rear suspension model consists of the truck arms, rear axle, panhard bar, and rear springs. The roll stiffness of the rear suspension is controlled primarily by the right/left coil springs that connect the truck arms to the chassis mounts and also by the flexibility of the truck arms themselves. In order to compare roll stiffness results with a rigid-body kinematics model developed in [8], the spring rates are set at (left rear = 325 lb/in, right rear = 350 lb/in. Rear roll stiffness is determined from a torque applied at the rear wheel hubs as shown in Figure 26. To model a rigid chassis, the coupled DOF between the suspension and chassis are restrained. The rear springs are restrained at the chassis connection in all three translations with free rotations. The connections between the truck arms and chassis mounts are modeled as ball joints, i.e. all rotational degrees of freedom are free, while all three translations are restrained. The panhard bar is modeled as a two-force member with ball joints at each end. In reality, the truck arm connections to the chassis are hinge joints, but to obtain results consistent with test data of rear suspension roll stiffness, they are modeled as ball joints. With this suspension geometry, spring rates, and truck arms, the roll stiffness of the rear suspension with a rigid chassis calculated from the FEM is K_R = 407 ft-lb/deg.

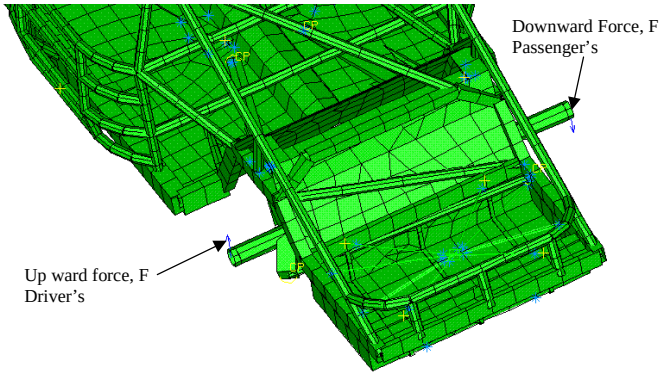

Figure 26. Applied Torque at the Rear Wheel Hub Centers

The rigid-body kinematics model [8] is unable to directly model the flexibility of the truck arms. Therefore, an auxiliary roll stiffness of the rear axle/truck arm assembly had to be determined from direct measurement of an actual suspension and input to the kinematics model. The total rear roll stiffness based on an auxiliary roll stiffness measured from a test car, and kinematics based on the above spring rates, resulted in a value of K_R = 402 ft-lb/deg. This roll-stiffness is within 2 % of the results from the finite element model.

The model of the pinned connection between the truck arms and chassis mounts is compared to a hinged joint model. At the mounting points, local coordinate systems are introduced to allow for rotation about axes oriented with small angles relative to the global lateral axis. To represent hinges, the rotational DOF about the local axis is free to rotate, while the other rotations and all translations are restrained in the local coordinate system. The roll stiffness of the full assembly with hinge joints is K_R = 463 ft-lb/deg, which is an increase of 14 % over the ball joint model. The rear roll stiffness values for the different models are compared in Table VII

Table VII. Summary of Rear Roll Stiffness Values. Spring rates (LR = 325 lb/in, RR = 350 lb/in)

Model	K (ft-lb/deg)
FEM (Ball Joints)	407
FEM (Hinge Joints)	463
Rigid Kinematics [8]	402

In order to determine the contribution of the rear axle/truck arm assembly to roll stiffness, the springs are removed from the model, and the roll stiffness is calculated with ball joints at the truck arm/chassis connection. In this way, the contribution to roll stiffness from the rear axle/truck arm assembly is determined without springs. The roll stiffness of this assembly is K_R = 127 ft-lb/deg, which is 31 % of the total rear roll stiffness. This value is consistent with an indirectly measured value of 112 ft-lb/deg reported for a “test” car given in [11].

ROLL STIFFNESS OF REAR SUSPENSION WITH FLEXIBLE CHASSIS

Effective rear roll stiffness of the suspension with flexible chassis is determined based on differential vertical load inputs at the rear wheel hub centers. For the rear roll stiffness calculation, only the rear suspension and chassis model is used while the front suspension is disconnected. The two front spring mounts are constrained in all translations and in y and z rotation. ($u_x = u_y = u_z = 0$, $\theta_z = \theta_y = 0$, and θ_x = free)

Table VIII compares the effective roll stiffness for the different chassis configurations. With the low spring rates used in the rear, the increase in chassis torsional stiffness has little effect (less than 2 %) on the change in rear suspension roll stiffness as expected.

Table VIII. Comparison Rear Suspension Roll Stiffness

Case	K_R Rear Roll stiffness ft-lb/deg	Increase over nominal (%)	Decrease from Rigid (%)
1	400	0.00	1.83
2	401	0.26	1.57
3	402	0.72	1.12
4	406	1.59	0.27
5	406	1.62	0.24
6	407	1.86	0.00
7	407	1.86	0.00
8	407	1.86	0.00
9	407	1.86	0.00

CONCLUSIONS

Finite element models have been constructed and assembled for the front and rear suspensions combined with the chassis of a Winston Cup racecar. Internal constraints between degrees-of-freedom at joints and internal releases have been modeled to simulate the connection between the chassis and suspension. The roll stiffness for the front and rear suspension finite element models were validated with a rigid-body kinematics model [8]. Torsional stiffness was increased by strategic modifications to the chassis structure. Effective front roll stiffness and camber response of the suspension with flexible chassis is determined based on differential vertical load inputs at the front wheel hub centers. The model allows for small deflections only and based on linear finite element analysis predicts changes in roll stiffness and camber response due to changes in chassis stiffness. Specifically, the vertical wheel travel allowed due to the vertical inputs is small resulting in camber and toe response due to changes in stiffness.

Major results from the study include the following:

- With the constraints used in this study, the minimum torsional stiffness required so that the effective roll stiffness of the front suspension is within 3 % from the roll stiffness with a rigid chassis, is about 23100 ft-lb/deg. This level of chassis torsional stiffness is sufficient to ensure that roll stiffness between sprung and unsprung masses is due almost entirely to the suspension.
- The change in camber follows the same trend as the effective roll stiffness. For a chassis stiffness of 23100 ft-lb/deg, the camber angles changed by approximately 11 % over the baseline chassis stiffness. The left and and right front tire camber change for configurations beyond this stiffness value are within 2.5 % of the the rigid chassis configuration. As the chassis stiffness is increased beyond 130% of nominal, both roll and camber do not change significantly. Thus it appears that a chassis stiffness of about 130% over nominal is sufficient to control both roll and camber.
- With low spring rates used in the rear suspension, the effective roll stiffness of the rear changes less than 2.2 % with over a 200 % increase in chassis stiffness. These results show that the effective roll stiffness of the rear suspension is minimally affected by chassis flexibility. With the magnitude of the baseline chassis torsional stiffness being over 15 times greater than the rear suspension roll stiffness, the chassis flexibility contributes insignificantly to the overall rear suspension/chassis roll stiffness.

The finite element model developed in this work is sufficiently accurate to determine the effects of global flexibility of the chassis on roll stiffness and camber response. However, the current stiffness model does not include details in the suspension pick-up brackets and supports, engine mounts and brackets, etc. In [9] a detailed model of the front suspension pick-up brackets is used to perform a detailed analysis of the local flexibility present at this critical area, and it's influence on roll stiffness and changes in camber response.

Useful future work would be to determine torsional stiffness of the chassis including the suspension by removing the sway bar, modeling infinite springs and loading differentially thru the wheel hubs instead of at the chassis spring mounts. Other useful measures would be to determine camber and toe response to a lateral force at the ground contact point. Using the finite element model developed in this work as a basis, we are currently performing analysis of these commonly used measures and will report results in a future manuscript.

ACKNOWLEDGEMENT

We would like to thank Kent Day for providing the suspension geometry data used in this work. We would also like to thank Greg Herrick and the reviewers of this manuscript for useful comments and suggestions.

REFERENCES

1. Martin, Gerald, “Revolution or Relic? Is Hendrick Motorsports’ Stiff Chassis Monte Carlo the Wave of the Future of Just Another Dinosaur?”, RACER Magazine, pp. 32-36, 1997.
2. Raju, Srikanth. “Design and Analysis of a Winston Cup Stock Car Chassis for Torsional Stiffness using the Finite Element Method”, Master of Science Thesis, Department of Mechanical Engineering, Clemson University, August 1998.
3. Keiner, Henning. “Static Structural Analysis of a Winston Cup Chassis under a Torsional Load”. Report # TR-95-100-ME-MSP. Department of Mechanical Engineering, Clemson University, 1995.
4. John Crawford, “Finite Element Analysis of a NASCAR Winston Cup Stock Car”, SAE Paper No. 942527, SAE Motorsports Engineering Conference, Detroit, MI, December 1994.
5. Lampert, Jon K. “Design and Analysis of a Twist Fixture to measure the Torsional Stiffness of a Winston Cup Chassis”, Master of Science Thesis, Department of Mechanical Engineering, Clemson University, August 1998.
6. NASCAR Winston Cup Rule Book, 1997.
7. Integrated Design Engineering Analysis Software Master Series 5, Computer Software. Structural Dynamics Research Corporation, 1997.
8. Day, Kent A. Doctor of Philosophy Dissertation. Department of Mechanical Engineering, Clemson University, in preparation.
9. Herrick, Gregory, P. “The Effects of Spring Perch Flexibility on Front Suspension Geometry and Roll Stiffness of a Winston Cup Stock Car Using the Finite Element Method”, Master of Science Thesis. Department of Mechanical Engineering, Clemson University, August 1998.
10. Soni, Pipasu H. “Effects of Chassis Flexibility on Roll Stiffness of a Winston Cup Stock Car Using the Finite Element Method”. Master of Science Thesis. Department of Mechanical Engineering, Clemson University, May 1998.
11. Day, Kent A., and Law, E. Harry. “Effects of Suspension Geometry and Stiffness Asymmetries on Wheel Loads During Steady Cornering for a Winston Cup Car”, SAE Motorsports Engineering Conference, SAE Paper No. 962531, 1996.